Immune Responses to Human Induced Pluripotent Stem Cells and their Derived Myogenic Progenitors Are Mediated by Different Mechanisms in Humanized Mice

Basma Benabdallah[1], Cynthia Désaulniers-Langevin[1], Marie-Lyn Goyer[1], Chloé Colas[1], Chantale Maltais[2], Yuanyi Li[1], Jean V. Guimond[3], Jacques P Tremblay[2], Elie Haddad[4] and Christian Beauséjour[1,5,*]

[1] Centre de recherche du CHU Ste-Justine, Montréal, Québec, Canada

[2] Centre de recherche du CHUQ, Université Laval, Québec, Canada

[3] CIUSSS du Centre-Sud-de-l'Ile-de-Montréal, Québec,Canada

[4] Département de Pédiatrie, Faculté de Médecine, Université de Montréal, Québec, Canada

[5] Département de pharmacologie et physiologie, Faculté de Médecine, Université de Montréal, Québec, Canada

* Correspondance:
Christian Beauséjour PhD
CHU Ste-Justine, 3175 Côte Sainte-Catherine
Montréal, Québec, Canada, H3T 1C5
(Phone) 514-345-4931 x4385
e-mail: c.beausejour@umontreal.ca

Running head: Immunogenicity of human iPSCs and their myogenic derived cells in mice

ABSTRACT

It is still unclear if immune responses will compromise the large scale utilization of cell therapies derived from human induced pluripotent stem cells (hiPSCs). To answer this question, we used humanized mouse models and evaluated the engraftment in skeletal muscle of myoblasts derived either directly from a muscle biopsy or differentiated from hiPSCs or fibroblasts. Our results showed that while allogeneic grafts were rejected, engraftment of autologous cells was tolerated, indicating reprogramming and differentiation procedures are not immunogenic. We also demonstrated that hiPSC-derived myogenic progenitors, in opposition to hiPSCs, are not targeted by natural killer (NK) cells both *in vitro* and *in vivo*. Yet, adoptive transfer of NK cells can prevent the formation of hiPSC-derived teratoma. Overall, our findings suggest that hiPSC-derived muscular therapies will be tolerated in presence of a competent human immune system and highlight the risk of forming a teratoma if using partially differentiated autologous human cells.

Words: 150

Key words: iPSC, humanized mice, adoptive transfer, myogenic cells, NK cells, T cells

Highlights:

1. hiPSC-derived myofibers are tolerated in autologous humanized mouse models
2. Infiltration of autologous T cells is not predictive of successful skeletal muscle engraftment
3. Adoptive transfer of NK cells prevents the formation of hiPSCs derived teratomas
4. NK cells are unable to reject established teratomas

INTRODUCTION

The potential of regenerative medicine is greatly enhanced by the development of human induced pluripotent stem cells (hiPSCs). Yet, the controversial possibility that hiPSC-derived cells arouse an autologous immune response could compromise their use in the clinic. Indeed, Zhao and colleagues were the first to observe that mouse iPSCs, but not embryonic stem cells (ESCs), are immunogenic when injected subcutaneously in syngeneic recipients, a response they latter showed was dependent on the presence of antigen presenting cells at the injection site (Todorova et al., 2016; Zhao et al., 2011). Subsequently, other studies have shown that mouse iPSC-derived cells can be immunogenic in syngeneic recipients and lead to the development of mechanisms similar to self-tolerance (Araki et al., 2013; de Almeida et al., 2014; Guha et al., 2013). In non-human primates, the transplantation of allogeneic, but not autologous, iPSC-derived neurons was shown to elicit an immune response in the brain (Emborg et al., 2013; Morizane et al., 2013).

Only one study has thus far addressed the *in vivo* immunogenicity of autologous hiPSCs and hiPSC-derived cells (Zhao et al., 2015). Immunogenicity was evaluated using humanized BLT mice (Hu-BLT), generated by the co-transplantation of hematopoietic stem cells along with human thymus tissues. The presence of thymic tissues allows for the development and maturation of competent human T cells making BLT mice a powerful model to study human immune responses (Brown et al., 2018; Shultz et al., 2012). Using this model, it was first showed that some tissues within teratomas derived from hiPSCs are immunogenic based on the infiltration of autologous human T cells (Zhao et al., 2015). It was also showed that autologous hiPSC-derived smooth muscle cells are immunogenic compared to hiPSC-derived retinal pigment epithelial cells which are not. Yet, the extent to which engrafted hiPSC-derived cells were

tolerated compared to hiPSC-derived allogeneic cells was not evaluated. In addition, the immunogenicity observed towards iPSC-derived smooth muscle cells was based solely on the infiltration of autologous T cells, and graft function or survival was not assessed. In another study, Kooreman and colleagues observed that mouse iPSCs and allogenic human ESC grafts were not rejected in Hu-BLT mice, suggesting that these mice may not be a sufficiently robust model to study the immunogenicity of hiPSCs and their derived cells (Kooreman et al., 2017).

BLT mice are deficient in functional NK cells presumably due to the absence of human IL-15, a cytokine necessary for their expansion and maturation (Carson et al., 1994). Hence, the *in vivo* contribution of the innate immunity, particularly the role of NK cells in the immunogenicity of hiPSCs and their derived cells remains largely unknown. Dressel and colleagues, previously showed that mouse iPSCs are highly susceptible targets of NK cells *in vitro* and in syngeneic mice (Dressel et al., 2010). They also showed that hiPSCs are the target of NK cells *in vitro* (Kruse et al., 2015). Whether hiPSCs and their derived cells are the target of NK cells *in vivo* has not been studied. To this end, using a combination of humanized mouse models (Hu-BLT and mice reconstituted following the adoptive transfer (AT) of adult PBMCs (herein referred as Hu-AT)) we provide evidence that skeletal muscle engraftment is not impaired despite low level autologous T cell infiltration. We also demonstrate a distinct role for NK cells in the immunogenicity of hiPSCs and their derived myogenic progenitors *in vitro* and *in vivo*.

RESULTS

Infiltration of autologous T cells in muscle does not mediate immune rejection in Hu-BLT mice

To evaluate the immunogenicity of skeletal muscle cell grafts, we used myoblasts either derived directly from a fetal muscle biopsy or myogenic progenitor cells (MPCs) differentiated from fetal liver fibroblasts (Figure 1A). MPCs were obtained using a two-step protocol as we previously described (Goudenege et al., 2012). Myoblasts and MPCs were highly positive for the myogenic marker CD56 and Desmin and were fully capable of forming myotubes *in vitro* (Figure S1A and S1B). Immunogenicity was determined by injecting cells into the *Tibialis anterior* of Hu-BLT mice reconstituted with either an allogeneic or autologous immune system (Figure S2A-C). Our results showed that four weeks after transplantation, muscle sections had a higher number of human dystrophin-expressing myofibers resulting from the fusion of autologous compared to allogeneic MPCs (Figures 1B and 1C). As expected, muscles injected with allogeneic MPCs were highly infiltrated with CD4 andCD8 T cells (Figure 1D). Surprisingly, engrafted autologous fibers were also infiltrated with T cells although at a lower level (Figure 1D). Importantly, the engraftment of MPCs was not impaired by the infiltration of autologous T cells as an equal number of fibers were formed when MPCs were transplanted in non-reconstituted immunodeficient NOD/SCID/IL2Rg null (NSG) mice (Figure 1C). The injection of the immunosuppressive drug FK506 to Hu-BLT mice prevented the rejection of allogeneic myoblasts, consistent with a T cell-dependent immune rejection mechanism (Figure S2D-F). In support of this observation, allogeneic but not autologous MPCs and myotubes were able to activate T cells *in vitro* when mixed with splenocytes collected from Hu-BLT mice (Figure 1E).

To determine if the infiltration of T cells was specific to the differentiation procedure of MPCs, we also transplanted muscles of Hu-BLT mice with myoblasts isolated directly from an

autologous fetal muscle biopsy. To our surprise, we also found muscles were infiltrated with CD8 T cells at a level similar to what we observed in muscles transplanted with autologous MPCs (Figures 1F and 1H). Again, the infiltration of T cells did not compromise engraftment of myoblasts in this model (Figures 1F and 1G). These results suggest that infiltration of autologous T cells should not be considered as a marker of MPCs rejection in skeletal muscles.

hiPSC-derived myofibers are not rejected following the AT of autologous PBMCs

The role of NK cells against hiPSCs and their derived cells has never been studied *in vivo*. Given Hu-BLT mice are deficient in functional NK cells, we choose to evaluate the immunogenicity of MPCs using a different humanized mouse model. To this end, we adoptively transferred NSG-SGM3 mice with human PBMCs (Hu-AT). We collected blood and skin fibroblasts from healthy adult donors and generated MPCs from fibroblast-derived hiPSCs (hiPSC-MPCs) using the same two-step differentiation protocol (Figure 2A). We choose to differentiate MPCs from hiPSCs, and not directly from fibroblasts, to better reflect future clinical settings and to evaluate immunogenicity potentially caused by both the reprogramming and differentiation procedures. We used an integration-free (Sendai virus) approach to generate hiPSC clones and then confirmed they had normal karyotypes and expressed the classical markers of pluripotency (Figure S3A and S3B and data not shown). Similar to what we observed in Hu-BLT mice, hiPSC-derived myofibers were mostly rejected four weeks following the AT of allogeneic but not autologous PBMCs (Figure 2B and 2C). Muscle tissues were highly infiltrated by both allogeneic or autologous T cells (Figure 2D). Yet, the infiltration of autologous immune cells had no impact on the graft as shown by the fact that the number of hiPSC-derived myofibers was not higher in non-reconstituted mice (Figure 2C). *In vitro*, hiPSC-MPCs and hiPSC-myotubes significantly

activated allogeneic but not autologous T cells in an MLR-like assay (Figure 2E and 2F). Conversely, NK cells purified from peripheral blood were effective in lysing, through degranulation, K562 or undifferentiated hiPSCs but were incapable of lysing hiPSC-MPCs (Figure 2G and 2H). These results are in line with the fact that hiPSCs, but not hiPSC-MPCs are deficient for the expression of the major histocompatibility complex I (MHC-I) and costimulatory molecules such as CD80, CD83 and CD86 (Figure S1C). Overall our results demonstrate that iPSC-derived muscular grafts are likely to be tolerated by autologous T cells, rejected by allogenic T cells and not the target of NK cells.

AT of NK cells prevents the formation of hiPSC-derived teratomas in mice

We then investigated if immune cells could protect against the formation of hiPSC-derived teratomas in an effort to predict the risk that injection of undifferentiated or partially differentiated cells could represent. We first determined if the AT of PBMCs could prevent the formation of teratomas derived from the injection of hiPSCs under the kidney capsule of NSG mice (Figure 3A and S4). Our results showed that, both autologous and allogeneic PBMCs were able to prevent the formation of hiPSC-derived teratomas (Figure 3B). To better define the role of T and NK cells in this process, we repeated the experiment using either NK-depleted PBMCs or purified NK cells. We found that the injection of autologous NK-depleted PBMCs was not able to prevent the growth of teratomas. This is in contrast to mice injected with allogeneic NK-depleted PBMCs which efficiently prevented to growth of teratomas, an effect likely meditated by allogeneic T cells. Moreover, we observed that teratomas that developed in absence of NK cells were significantly larger in size compared to teratomas grown in absence of immune cells (Figure 3C). We speculate that their enhanced growth was fueled by human cytokines secreted by

autologous PBMCs. Importantly, our results also showed that the injection of purified NK cells alone was able to prevent the formation of hiPSC-derived teratomas in both autologous or allogeneic settings (Figure 3B). This suggests that NK cells, but not autologous T cells, are efficient in preventing the development of hiPSC-derived teratomas. As expected and in support of these results, we observed that the Hu-BLT mice, which do not have functional NK cells, could not prevent the growth of hiPSC-derived teratomas (Figure 3D and 3E). Still, teratomas were found infiltrated with low level, non-randomly distributed autologous T cells (Figure 3F), supporting the findings by Zhao and colleagues (Zhao et al., 2015). This is in contrast to hiPSCs injected in Hu-BLT mice, reconstituted with an allogeneic immune system, in which the growth of teratomas was partially inhibited (50%) and were residual teratomas were massively infiltrated by T cells and undergoing apoptosis (Figure 3F).

AT of NK cells fails to reject established teratomas in mice

To further evaluate the role of NK cells, we repeated the above-described experiment but this time we injected immune cells six weeks after the injection of hiPSCs, a time at which teratomas had already started to grow and cells to differentiate (Figure 4A). While we found that allogeneic PBMCs or NK-depleted PBMCs were capable of rejecting teratomas, autologous PBMCs and purified NK cells were not (Figure 4B). Analysis of the immune infiltrate within teratomas showed a massive T cell infiltration and apoptosis in remaining allogeneic tissues (Figure 4C). In comparison, only few T cells were found in autologous teratomas. Virtually no NK cells were found in growing teratomas suggesting these cells lose their ability to recognize differentiated or partially differentiated hiPSC-derived cells. This is supported by the fact that cells within a teratoma were found to express MHC-I and that hiPSCs are capable of expressing MHC-I

molecules within a few hours after being placed in presence of serum *in vitro* (Figure S3C). Overall, these results indicate that while NK cells are very effective at preventing the formation of a teratoma from hiPSCs, they lose this ability against differentiated or partially differentiated cells.

DISCUSSION

The ability to generate hiPSCs at an affordable cost and in a timely manner will be necessary to assure the success of future hiPSC-derived cell therapies. Moreover, it will be essential to demonstrate that hiPSC-derived cells, whether obtained from autologous donors or through the development of universal cell lines (Liang et al., 2018), are safe and tolerated by human immune cells. Using two distinct humanized mouse models, we here provide evidence that MPCs are tolerated by autologous T and NK cells. Our observation that MPCs attract autologous CD8+ T cells at a level similar to that of myoblasts derived from a muscle biopsy, yet without compromising engraftment, was surprising. Our hypothesis is that T cells may have been attracted by bovine serum proteins and/or an altered secretory phenotype acquired during the short *in vitro* growth expansion period of MPCs. Another possibility is that aberrantly expressed antigens may have attracted and induced tolerance/exhaustion of infiltrating autologous T cells. Unfortunately, the low level of infiltrating T cells prevented us from testing this hypothesis. Moreover, the different differentiation protocols already published for the generation of MPCs from iPSCs will also need to be evaluated for their ability to evade the immune system (Chan et al., 2018; Shelton et al., 2016; van der Wal et al., 2018). It also remains to be determined if the presence of autologous T cells can impact long-term engraftment (more than 4 weeks). Indeed, 4 weeks after the AT of PBMCs, we observed equal infiltration of T cells in both autologous and

allogeneic conditions (Figure 2D), suggesting mice were at the early stage of graft-versus-host disease. The use of NSG mice that lack the murine MHC allowing to evade graft-versus-host disease but that retain T cell function upon engraftment will likely help to overcome this issue (Brehm et al., 2018). Our results also provide the first evidence that hiPSC-derived MPCs, unlike hiPSCs, are not the target of NK cells *in vivo*. Indeed, we believe there was a sufficient number of NK cells injected in Hu-AT mice to efficiently reject MPC-derived fibers. This is based on the fact that the injection of a similar number of NK cells was able to prevent the growth of teratomas in the same model. Our results also demonstrated that hiPSCs are the target of NK cells in Hu-AT mice, which we showed prevented the formation of teratomas. Overall, our study provides essential pre-clinical data supporting the usage of iPSC-derived MPCs in regenerative medicine and demonstrate that only undifferentiated iPSCs are the target of human NK cells *in vivo*.

ACKNOWLEDGMENTS

We are grateful to the flow cytometry and animal facility for providing technical support and to Renée Dicaire for handling clinical samples. This work was supported by a grant from the Canadian Institute of Health Research #MOP-126096 to C.M.B., E. H. and J.P.T., by a grant from le réseau ThéCell from the Fonds de la recherche du Québec – Santé (FRQS) and the support from la Fondation Charles Bruneau for access to technological platforms. C.M.B. was supported by a senior scientist award from the FRQS.

AUTHOR CONTRIBUTIONS

B.B., C.D.L., M.L.G., C.C., Y.L. and C.M. performed experiments. B.B., H.E. and C.B. designed the studies, J.V.G. provided cells, J.P.T. provided cells, reagents and expertise. B.B. and C.B. wrote the manuscript.

CONFILCT OF INTEREST STATEMENT

The authors declare no competing interests

REFERENCES

Araki, R., Uda, M., Hoki, Y., Sunayama, M., Nakamura, M., Ando, S., Sugiura, M., Ideno, H., Shimada, A., Nifuji, A.*, et al.* (2013). Negligible immunogenicity of terminally differentiated cells derived from induced pluripotent or embryonic stem cells. Nature *494*, 100-104.

Brehm, M.A., Kenney, L.L., Wiles, M.V., Low, B.E., Tisch, R.M., Burzenski, L., Mueller, C., Greiner, D.L., and Shultz, L.D. (2018). Lack of acute xenogeneic graft- versus-host disease, but retention of T-cell function following engraftment of human peripheral blood mononuclear cells in NSG mice deficient in MHC class I and II expression. FASEB J, fj201800636R.

Brown, M.E., Zhou, Y., McIntosh, B.E., Norman, I.G., Lou, H.E., Biermann, M., Sullivan, J.A., Kamp, T.J., Thomson, J.A., Anagnostopoulos, P.V.*, et al.* (2018). A Humanized Mouse Model Generated Using Surplus Neonatal Tissue. Stem Cell Reports *10*, 1175-1183.

Carson, W.E., Giri, J.G., Lindemann, M.J., Linett, M.L., Ahdieh, M., Paxton, R., Anderson, D., Eisenmann, J., Grabstein, K., and Caligiuri, M.A. (1994). Interleukin (IL) 15 is a novel cytokine that activates human natural killer cells via components of the IL-2 receptor. J Exp Med *180*, 1395-1403.

Chan, S.S., Arpke, R.W., Filareto, A., Xie, N., Pappas, M.P., Penaloza, J.S., Perlingeiro, R.C.R., and Kyba, M. (2018). Skeletal Muscle Stem Cells from PSC-Derived Teratomas Have Functional Regenerative Capacity. Cell Stem Cell *23*, 74-85 e76.

de Almeida, P.E., Meyer, E.H., Kooreman, N.G., Diecke, S., Dey, D., Sanchez-Freire, V., Hu, S., Ebert, A., Odegaard, J., Mordwinkin, N.M.*, et al.* (2014). Transplanted terminally differentiated induced pluripotent stem cells are accepted by immune mechanisms similar to self-tolerance. Nat Commun *5*, 3903.

Dressel, R., Nolte, J., Elsner, L., Novota, P., Guan, K., Streckfuss-Bomeke, K., Hasenfuss, G., Jaenisch, R., and Engel, W. (2010). Pluripotent stem cells are highly susceptible targets for syngeneic, allogeneic, and xenogeneic natural killer cells. FASEB J *24*, 2164-2177.

Emborg, M.E., Liu, Y., Xi, J., Zhang, X., Yin, Y., Lu, J., Joers, V., Swanson, C., Holden, J.E., and Zhang, S.C. (2013). Induced pluripotent stem cell-derived neural cells survive and mature in the nonhuman primate brain. Cell reports *3*, 646-650.

Goudenege, S., Lebel, C., Huot, N.B., Dufour, C., Fujii, I., Gekas, J., Rousseau, J., and Tremblay, J.P. (2012). Myoblasts Derived From Normal hESCs and Dystrophic hiPSCs Efficiently Fuse With Existing Muscle Fibers Following Transplantation. Molecular therapy : the journal of the American Society of Gene Therapy *20*, 2153-2167.

Guha, P., Morgan, J.W., Mostoslavsky, G., Rodrigues, N.P., and Boyd, A.S. (2013). Lack of immune response to differentiated cells derived from syngeneic induced pluripotent stem cells. Cell Stem Cell *12*, 407-412.

Kooreman, N.G., de Almeida, P.E., Stack, J.P., Nelakanti, R.V., Diecke, S., Shao, N.Y., Swijnenburg, R.J., Sanchez-Freire, V., Matsa, E., Liu, C.*, et al.* (2017). Alloimmune Responses of Humanized Mice to Human Pluripotent Stem Cell Therapeutics. Cell reports *20*, 1978-1990.

Kruse, V., Hamann, C., Monecke, S., Cyganek, L., Elsner, L., Hubscher, D., Walter, L., Streckfuss-Bomeke, K., Guan, K., and Dressel, R. (2015). Human Induced Pluripotent Stem Cells Are Targets for Allogeneic and Autologous Natural Killer (NK) Cells and Killing Is Partly Mediated by the Activating NK Receptor DNAM-1. PLoS One *10*, e0125544.

Liang, Q., Monetti, C., Shutova, M.V., Neely, E.J., Hacibekiroglu, S., Yang, H., Kim, C., Zhang, P., Li, C., Nagy, K.*, et al.* (2018). Linking a cell-division gene and a suicide gene to define and improve cell therapy safety. Nature *563*, 701-704.

Morizane, A., Doi, D., Kikuchi, T., Okita, K., Hotta, A., Kawasaki, T., Hayashi, T., Onoe, H., Shiina, T., Yamanaka, S.*, et al.* (2013). Direct comparison of autologous and allogeneic transplantation of iPSC-derived neural cells in the brain of a non-human primate. Stem Cell Reports *1*, 283-292.
Shelton, M., Kocharyan, A., Liu, J., Skerjanc, I.S., and Stanford, W.L. (2016). Robust generation and expansion of skeletal muscle progenitors and myocytes from human pluripotent stem cells. Methods *101*, 73-84.
Shultz, L.D., Brehm, M.A., Garcia-Martinez, J.V., and Greiner, D.L. (2012). Humanized mice for immune system investigation: progress, promise and challenges. Nat Rev Immunol *12*, 786-798.
Todorova, D., Kim, J., Hamzeinejad, S., He, J., and Xu, Y. (2016). Brief Report: Immune Microenvironment Determines the Immunogenicity of Induced Pluripotent Stem Cell Derivatives. Stem Cells *34*, 510-515.
van der Wal, E., Herrero-Hernandez, P., Wan, R., Broeders, M., In 't Groen, S.L.M., van Gestel, T.J.M., van, I.W.F.J., Cheung, T.H., van der Ploeg, A.T., Schaaf, G.J.*, et al.* (2018). Large-Scale Expansion of Human iPSC-Derived Skeletal Muscle Cells for Disease Modeling and Cell-Based Therapeutic Strategies. Stem Cell Reports *10*, 1975-1990.
Zhao, T., Zhang, Z.N., Rong, Z., and Xu, Y. (2011). Immunogenicity of induced pluripotent stem cells. Nature *474*, 212-215.
Zhao, T., Zhang, Z.N., Westenskow, P.D., Todorova, D., Hu, Z., Lin, T., Rong, Z., Kim, J., He, J., Wang, M.*, et al.* (2015). Humanized Mice Reveal Differential Immunogenicity of Cells Derived from Autologous Induced Pluripotent Stem Cells. Cell Stem Cell *17*, 353-359.

FIGURE LEGENDS

Figure 1. Infiltration of autologous T cells in muscles does not prevent engraftment of myogenic cells in Hu-BLT mice

(A) Schematic of the BLT humanized mouse model (Hu-BLT). NSG mice were transplanted with human fetal thymus and autologous liver-derived $CD34^+$ cells. At week 10 (W10) post immune reconstitution, human myogenic progenitor cells (MPCs) derived from fetal liver fibroblasts or myoblasts isolated directly from a fetal muscle biopsy were injected in the skeletal muscle of Hu-BLT. Mice were sacrificed 4 weeks later, and muscles were harvested and analyzed for cell engraftment and infiltration of immune cells.

(B) Representative photos of muscle sections from Hu-BLT mice showing increased engraftment of autologous compared to allogeneic human MPC-derived dystrophin positive fibers (in red). DAPI staining was performed to visualize nuclei (in blue). Showed are photos taken at 20X. Scale bar, 100 µm.

(C) Counts of human dystrophin positive fibers observed in muscle sections of Hu-BLT mice transplanted with MPCs as shown in panel B. Also showed are counts in non-immune reconstituted NSG mice to assess overall engraftment potential of the different donors. Each dot represents the mean ± SEM number of dystrophin positive fibers from three to five randomly selected fields per mouse.

(D) Representative photos showing CD4+ and $CD8^+$ T cell infiltration (in red) in muscle sections of Hu-BLT mice transplanted with autologous or allogeneic MPCs. DAPI staining was performed to visualize nuclei (in blue). Showed are photos taken at 20X. Scale bar, 100 µm.

(E) Splenocytes were collected from Hu-BLT mice 10 weeks after immune reconstitution, and the activation of T cells (as determined by gating $CD3^+/CD69^+$ cells) was measured after a co-culture with autologous or allogeneic MPCs or myotubes (ratio 1:2) for 3 days. PHA was used as a positive control. Shown is the mean ± SEM of 2 independent experiments done in triplicate using splenocytes collected from 2 different mice.

(F) Representative photos of muscle sections from Hu-BLT mice showing engraftment of autologous human fetal myoblast-derived dystrophin positive fibers and CD8 T cell infiltration (in red). DAPI staining was performed to visualize nuclei (in blue). Showed are photos taken at 20X. Scale bar, 100 µm.

(G) Counts of human dystrophin-positive fibers observed in muscle sections of Hu-BLT mice transplanted with autologous fetal myoblast as shown in panel E. Also showed are counts in non-immune reconstituted NSG mice to assess overall engraftment potential of the donor. Each dot represents the mean number of dystrophin-positive fibers from three to five randomly selected fields per mouse.

(H) Frequency of CD8 T cells infiltrated in muscle of Hu-BLT mice as shown in panels D and E. Each dot represents the mean number of T cells in three to five randomly selected fields per mouse.

Figure 2. iPSC-derived myofibers are not rejected in Hu-AT mice.

(A) Schematic of the humanized mouse model generated following the AT (Hu-AT) of human PBMCs. NSG-SGM3 mice were transplanted on day 0 (D0) with hiPSC-derived MPCs and either autologous or allogeneic PBMCs. Mice were sacrificed 4 weeks later, and skeletal muscles were harvested and analyzed for cell engraftment and infiltration of immune cells.

(B) Representative photos of muscle sections from Hu-AT mice showing increased engraftment of autologous compared to allogeneic hiPSC-MPCs-derived dystrophin positive fibers (in red). DAPI staining was performed to visualize nuclei (in blue). Showed are photos taken at 10X. Scale bar, 20 µm.

(C) Counts of human dystrophin positive fibers observed in muscle sections of Hu-AT mice transplanted with hiPSC-MPCs as shown in panel B. Also showed are counts in non-immune reconstituted NSG mice to assess overall engraftment potential of the donor. Each dot represents the mean ± SEM number of dystrophin positive fibers from three to five randomly selected fields per mouse.

(D) Representative photos showing CD4+, $CD8^+$ T cell and $NKp46^+$ NK cell infiltration (in red) in muscle sections of Hu-AT mice transplanted with autologous or allogeneic PBMCs. DAPI staining was performed to visualize nuclei (in blue). Showed are photos taken at 20X. Scale bar, 100 µm.

(E, F) Measures of T cell activation (as determined by gating for $CD3^+/CD69^+$ cells) after co-culture of hiPSC-derived MPCs or myotubes with allogeneic or autologous PBMCs for 3 days. OKT3 was used as a positive control. Shown is the mean ± SEM of 2 independent experiments done in triplicate using cells collected from 2 different donors.

(G) hiPSCs but not hiPSC-MPCs induce degranulation of NK cells *in vitro*. Degranulation was determined by evaluating CD107 expression on gated $CD3^-/CD56^+$ NK cell populations after a 4 hour co-culture between freshly isolated PBMCs and hiPSCs or hiPSC-MPCs (ration 1:2). K562 cells were used as a positive control. Shown is the mean ± SEM of 2 independent experiments done in triplicate using cells collected from 2 different donors.

(H) hiPSCs but not hiPSC-MPCs are lysed by purified NK cells *in vitro*. Cell lysis was determined by flow cytometry with the absolute count of PKH26-stained hiPSCs or hiPSC-MPCs after a 4 hour co-culture with NK cells purified by magnetic negative selection. K562 cells were used as a positive control. Shown is the mean ± SEM of 2 independent experiments done in triplicate using cells collected from 2 different donors.

Figure 3. NK cells are sufficient to prevent the formation of hiPSC-derived teratomas in mice.

(A) Timeline of cell injection. PBMCs, NK-depleted PBMCs or purified NK cells were intravenously injected at day 0 (DO) to generate Hu-AT mice. Autologous or allogeneic hiPSCs were transplanted under the kidney capsule on the same day. The incidence of teratomas was evaluated 8 weeks after the injection of immune cells.

(B) Incidence of teratomas after the AT of the indicated immune cells in NSG mice. Shown is the proportion of teratomas derived from the indicated hiPSCs clones and their relative sizes. na= not applicable.

(C) Representative photos showing the increased size of teratomas isolated from NSG mice immune-reconstituted with NK-depleted autologous PBMCs compared to control non-reconstituted mice.

(D) Timeline of the injection of hiPSCs in Hu-BLT mice. NSG mice were injected with fetal tissues as previously described. 8 weeks later (W8), mice were injected with hiPSCs derived from autologous or allogeneic fetal liver fibroblasts. Teratomas were allowed to grow for 8 weeks before mice were sacrificed at week 16 (W16).

(E) Incidence of teratomas in Hu-BLT mice. Shown is the proportion of teratomas derived from the indicated hiPSCs clones and their relative infiltration by T cells. na = not applicable.

(F) Representative photos showing the extensive infiltration of $CD4^+$ and $CD8^+$ T cells (in red) and apoptosis (as determined by TUNEL in green) in sections of teratomas collected from Hu-BLT mice

injected with allogeneic but not autologous hiPSCs. DAPI staining was performed to visualize nuclei (in blue). Showed are photos taken at 20X. Scale bar, 100 µm.

Figure 4. Established teratomas are not the target of NK cells in Hu-mice.

(A) Timeline of cell injection. NSG mice were first injected under the kidney capsule with hiPSCs. 6 weeks later (W6), mice were injected intravenously with PBMCs, NK-depleted PBMCs or purified NK cells. 2 weeks after the AT of immune cells (W8), mice were sacrificed and the incidence of teratomas and the infiltration of immune cells determined.

(B) Incidence of teratomas in the kidney capsule of Hu-AT mice. Shown is the proportion of teratomas derived from the indicated hiPSCs clones and their relative infiltration by T and NK cells. na = not applicable.

(C) Representative photos showing the extensive infiltration of $CD4^+$ and $CD8^+$ T cells (in red) and apoptosis (as determined by TUNEL in green) in sections of teratomas collected from Hu-AT mice injected with allogeneic but not autologous PBMCs. DAPI staining was performed to visualize nuclei (in blue). Showed are photos taken at 20X. Scale bar, 100 µm.

EXPERIMENTAL PROCEDURES

Humanized mice

NOD/SCID/IL2Rγ null (NSG) and NSG-SGM3 (expressing human IL3, GM-CSF and SCF) mice were obtained from the Jackson Laboratory (Bar Harbor, ME) and housed in the animal care facility at the CHU Sainte-Justine Research Center under pathogen-free conditions in sterile ventilated racks. All *in vivo* manipulations were previously approved by the institutional committee for good laboratory practices for animal research (protocol #579). BLT humanized mice (Hu-BLT) were generated by surgical implantation of small pieces (1-2 mm^3) of human fetal thymus tissues under the kidney capsule and intravenous delivery of $CD34^+$ hematopoietic stem cells isolated from autologous fetal liver into six week-old NSG mice previously irradiated with 2 Gy total body irradiation (1 Gy/min using a Faxitron CP-160) as previously described (Shultz et al., 2012). Fetal tissues were obtained from consented healthy donors after surgical abortion at around week 20 of pregnancy. To monitor the human immune cell engraftment in humanized mice, peripheral blood was collected and leukocytes were purified using a red blood cell lysis solution. Cells were then labeled with conjugated antibodies for human APC-CD45, BB515-CD3, APC-H7-CD19, and PE-CD8 (all from BD Biosciences) and analyzed by flow cytometry (BD FACSCANTO II, BD Biosciences). For adoptive transfer experiments, human adult blood was collected and immune cells purified by Ficoll (GE healthcare). Mice were injected i.v. with 10 million freshly isolated PBMCs or NK-depleted PBMCs obtained from the negative fraction of a positive selection (CD56+) kit (STEMCELL Technologies). Alternatively, mice were injected with 0.5-1.5 million NK cells purified using the NK cell enrichment negative selection kit (STEMCELL Technologies).

Generation and characterization of iPSCs

Fibroblasts isolated either from human fetal liver tissues or human skin after collagenase dissociation were reprogrammed into hiPSCs with the integration-free based Sendai virus (Cytotune 2.0 kit from Life Technologies). Fibroblasts were used at low population doubling to increase efficiency of reprogramming. Emerging colonies from transduced cells were manually picked and cultured under feeder-free conditions in Essential 8 medium on Geltrex-coated dishes (Life Technologies). hiPSC clones were passaged at least 15 times to increase stable pluripotency. hiPSC generation and characterization were done in the iPSC – cell reprogramming core facility

of CHU Sainte-Justine. hiPSC colonies were stained with the antibodies for anti-human SSEA-4, Sox2, OCT4 and TRA1-60 overnight at 4°C using the pluripotent Stem Cell 4-Marker Immunocytochemistry Kit (Life Technologies), followed by incubation with an ALEXA secondary antibodies for 30 minutes at room temperature. Nuclei were counterstained with DAPI.

Differentiation into myogenic progenitor cells

Myogenic progenitor cells (MPCs) were generated either directly from fibroblasts, or following fibroblast reprogramming into hiPSCs (hiPSC-MPCs). Differentiation of fibroblasts into MPCs was obtained after transduction with a MyoD-expressing adenovirus for five hours at MOI 3. hiPSC-MPCs were differentiated by first culturing hiPSC colonies in MB1 myogenic medium (Hyclone) supplemented with 10 ng/ml of bFGF for five days on Geltrex-coated culture dishes and then transduced with a MyoD-expressing adenovirus as described above (Goudenege et al., 2012). Both MPCs and hiPSC-MPCs were used the day after transduction to avoid premature fusion of the cells.

Splenocyte and T cell activation assays

Splenocytes and PBMCs were isolated from Hu-BLT mice following mechanical digestion of the spleen or isolation using Ficoll respectively. Effector cells (splenocytes or PBMCs) were then co-cultured with either autologous or allogeneic MPCs or myotubes at 1:2 ratio during three days at 37˚C. Effector cells were added to MPCs directly after transduction with MyoD or after a five day culture in 2% fetal bovine serum to allow the formation of myotubes. T cell activation was measured with a PE-conjugated anti-hCD69 on $CD3^+$ gated viable cells by flow cytometry (BD LSRFortessa, BD Biosciences). Effector cells without stimulation were used as a negative control, and PHA or an anti-CD3 (OKT3) antibody were used as positive controls. 7-AAD (BD Biosciences) was used to exclude dead cells.

NK cell degranulation and cytotoxicity assays

Freshly purified NK cells (as described above) were incubated with or without target cells at the indicated ratios. K562 cells were used as a positive control in all experiments. For the NK cell degranulation assay, effector and target cells were co-cultured at 1:2 ratio in the presence of FITC-conjugated anti-human CD107a/b for one hour at 37˚C, then 2µl/ml of monensin (BD

Biosciences) was added to the cell mixture for an additional three hours of incubation. For cytotoxicity assay, effector and PKH26-stained target cells were mixed at 1:1 or 5:1 ratio and incubated for four hours at 37˚C. At the end of the incubation, degranulation was quantified by flow cytometry (BD LSRFortessa, BD Biosciences) after gating on CD3-/CD56+/CD107+ viable cells and the extent of cytotoxicity was determined by the relative number of live target cells labelled with PKH26 only and dead cells labelled with both PKH26 (Sigma-Aldrich) and 7-AAD (BD Biosciences).

Fetal fibroblast and myoblast isolation: Fetal muscle and liver biopsies were minced into small pieces and digested using a solution of PBS with 0.2% of collagenase (Roche) and 0.25% of dispase (STEMCELL technologies) at 37˚C during 30 minutes with manual intermittent mixing. Myoblasts and fibroblasts were then cultured and expanded respectively in myogenic MB1 medium and 10% fetal bovine serum-supplemented DMEM.

Intramuscular transplantation of myogenic cells

Tibialis anterior (TA) muscle of mice were implanted with one million myogenic cells (either myoblasts, MPCs or hiPSC-MPCs) in 20 µl of PBS containing 10 µg/ml of cardiotoxin (Sigma). The grafted *TA* muscles were harvested four weeks after transplantation and frozen in optimal cutting temperature compound (OCT, VWR). Cryosections of transplanted muscles were immunostained with antibodies against human dystrophin (Developmental Studies Hybridoma Bank, University of Iowa) and human CD4 and CD8 (both from Biolegend).

Teratoma formation

Approximately one million iPSCs were first detached in cell clumps using gentle cell dissociation reagent (STEMCELL Technologies) and resuspended in PBS containing 50% of Geltrex. Cells were then injected unilaterally under the kidney capsule of mice. Eight weeks later, teratomas were dissected out and placed in OCT. Cryosections were stained with hematoxylin eosin for histological analysis, and immunostained with antibodies against human CD4, CD8 (all from Biolegend) and TUNEL (Roche).

MPC characterization and differentiation *in vitro*: MPCs cultured in MB1 were fixed and permeabilized using ethanol 95% and immunostained with a mouse anti-human desmin antibody (1:200 from DAKO) overnight at 4˚C and an anti-mouse ALEXA fluor 594 (1:500 from Invitrogen) at room temperature for one hour. Confluent MPCs were maintained in Dulbecco's modified Eagle's medium (DMEM) supplemented with 2% fetal bovine serum and antibiotics for three-five days. Myotubes were then immunostained with a mouse anti-MyHC antibody (1:100 from the Developmental Studies Hybridoma Bank, University of Iowa) for two hours at room temperature and an anti-mouse ALEXA fluor 594 (1:500) at room temperature for one hour. Nuclei were counterstained with DAPI. Cells were then phenotypically characterized by flow cytometry (BD LSRFortessa, BD Biosciences) using conjugated antibodies against HLA-I, CD80, CD83, CD86, MICA/B and CD112/155 (all from BD Biosciences).

Statistical Analysis

GraphPad Prism 8 software was used for statistical analysis; ρ values on multiple comparisons were calculated using Student's t-Tests or One-way analysis of variance (ANOVA) with Bonferroni post Hoc test. *$p<0.05$, **$p<0.01$, ****$p<0.0001$.

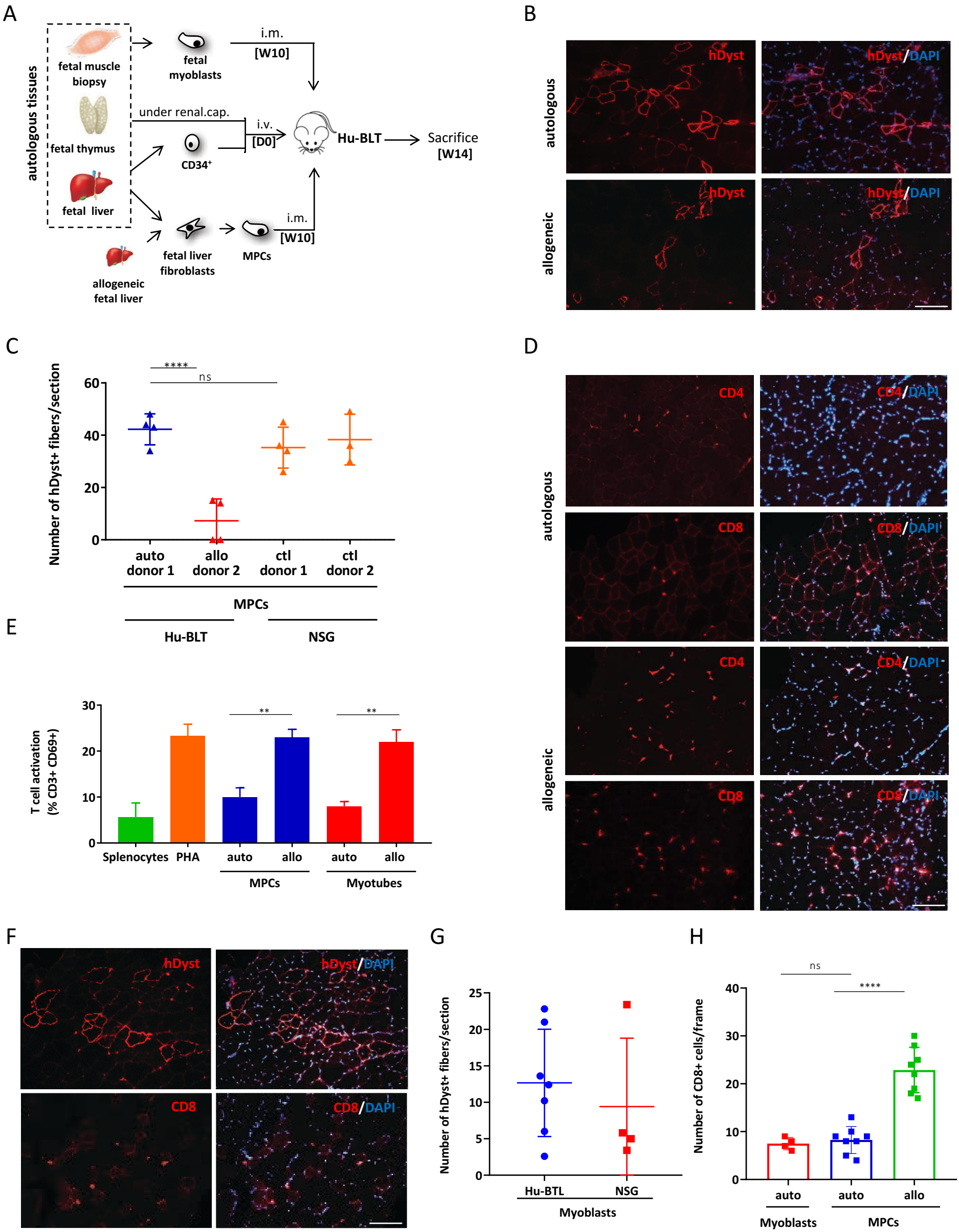

Benabdallah et al. Figure 1

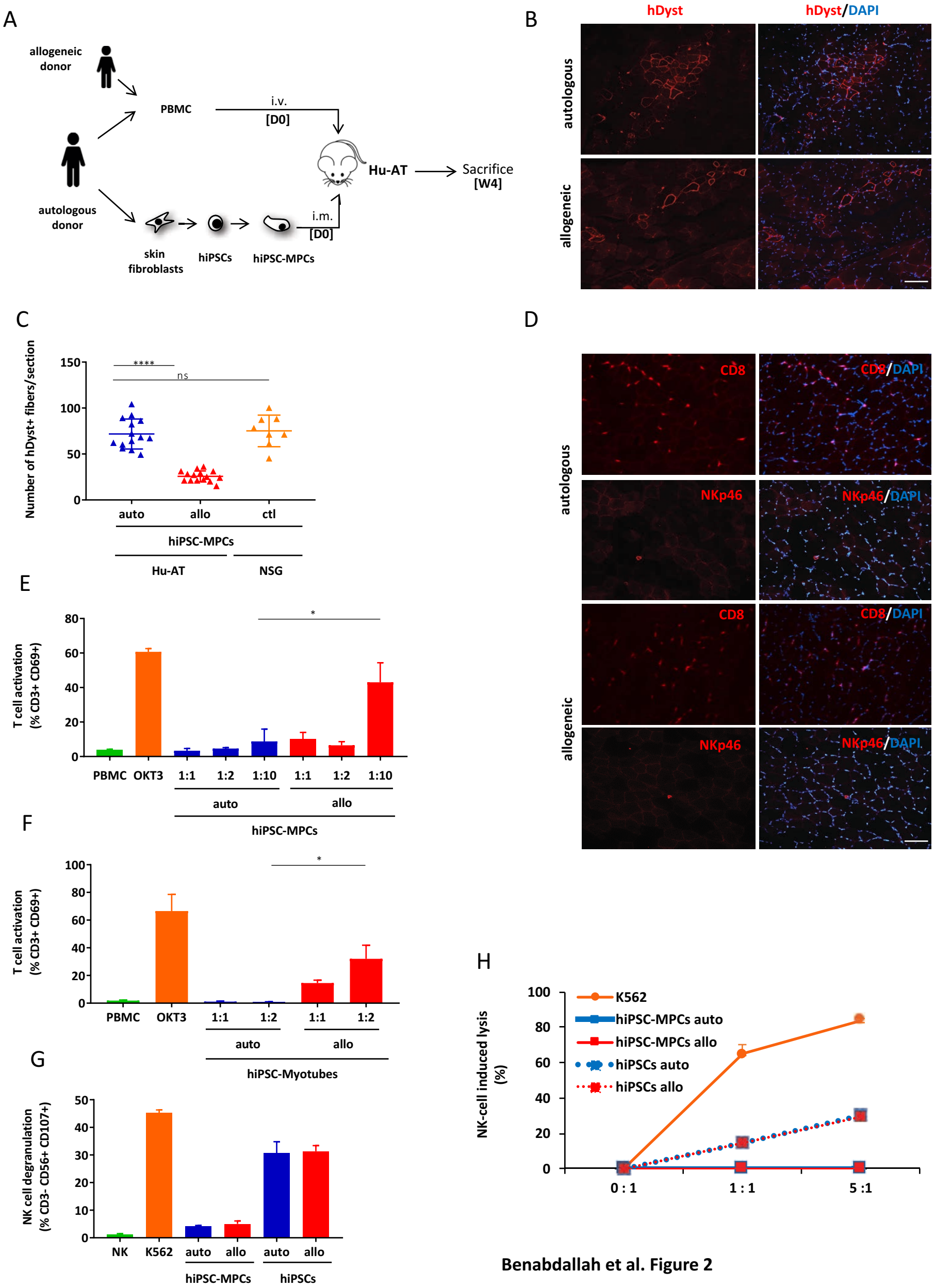

Benabdallah et al. Figure 2

A

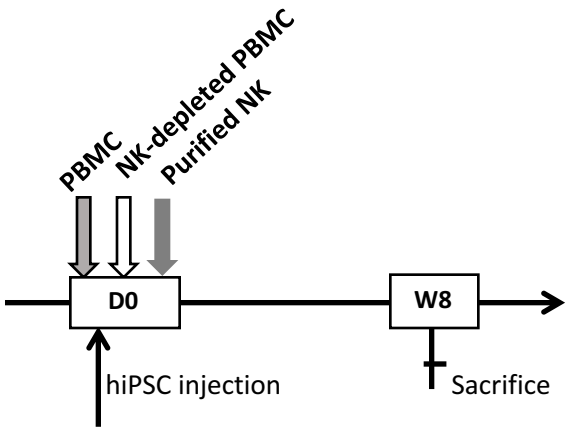

B

Groups		hiPSC Clones	Teratoma formation
NSG		CB C1	4/5
		GH C4	3/3
		SL C5	3/4
		Total	10/12 (83%)
Hu-AT (PBMC)	Autologous	CB C1	0/2
		GH C4	0/3
		CB C5	1/4
		Total	1/9 (11%)
	Allogeneic	SL C1	0/2
		SL C5	0/2
		Total	0/4 (0%)
Hu-AT (NK-depleted PBMC)	Autologous	CB C1	4/4
		CB C5	3/3
		Total	7/7 (100%)
	Allogeneic	SL C5	0/4
		SL C1	0/3
		Total	0/7 (0%)
Hu-AT (Purified NK)	Autologous	CB C1	0/3
		GH C4	0/3
		Total	0/6 (0%)
	Allogeneic	CB C7	0/5
		CB C7	0/6
		Total	0/11 (0%)

C

Groups	Teratomas
NSG	
Hu-AT (NK-depleted autologous PBMC)	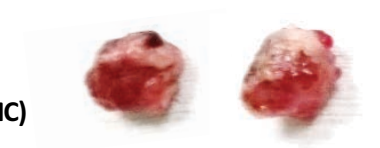

D

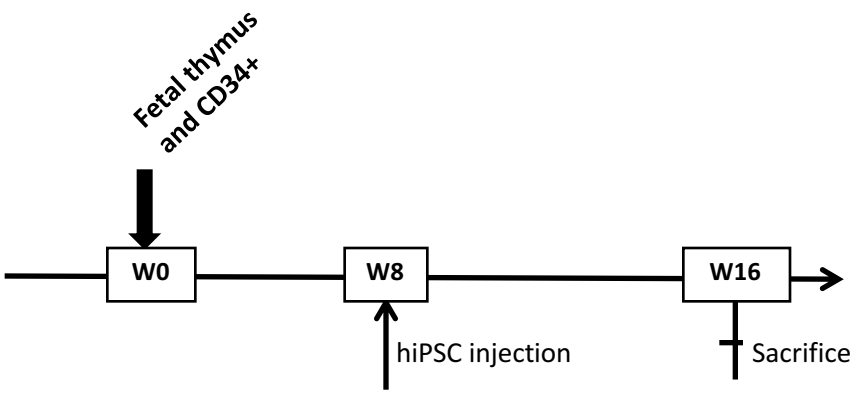

E

Groups		hiPSC Clones	Teratoma formation	T cell infiltration
NSG		23-16	4/4	na
		CB C1	4/4	
		Total	8/8 (100%)	
Hu-BLT	Autologous	23-16	5/6	+
		Total	5/6 (83%)	
	Allogeneic	CB C1	2/2	++++
		CB C1	1/4	
		Total	3/6 (50%)	

F

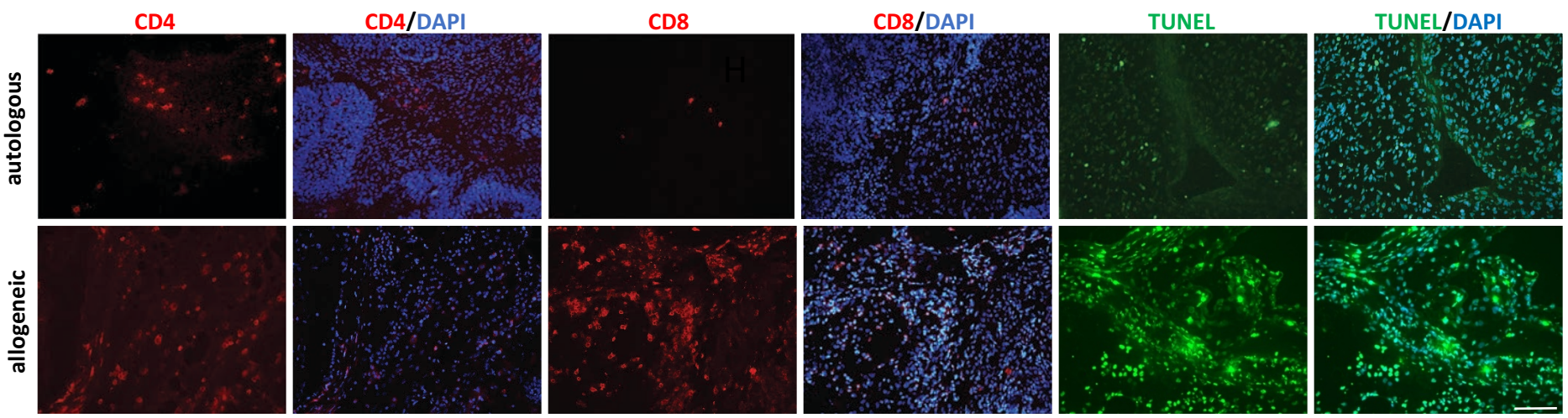

Benabdallah et al. Figure 3

A

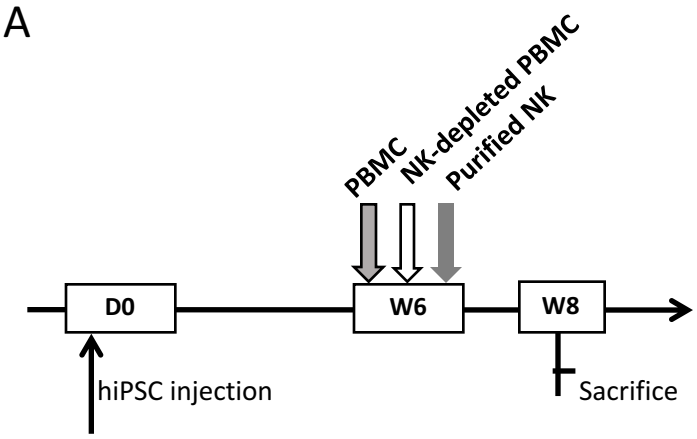

B

Groups		hiPSC Clones	Teratoma formation	T cell infiltration	NK cell infiltration
NSG		CB C1	4/4	na	na
		SL C1	3/3		
		Total	7/7 (100%)		
Hu-AT (PBMC)	Autologous	CB C1	4/4	+	+
		CB C1	2/4		
		Total	6/8 (75%)		
	Allogeneic	SL C1	0/3	++++	+
		CB C1	1/4		
		Total	1/7 (14%)		
Hu-AT (NK-depleted PBMC)	Allogeneic	CB C1	1/8	++++	na
		Total	1/8 (12%)		
Hu-AT (Purified NK)	Allogeneic	CB C1	7/8	na	+
		Total	7/8 (87%)		

C

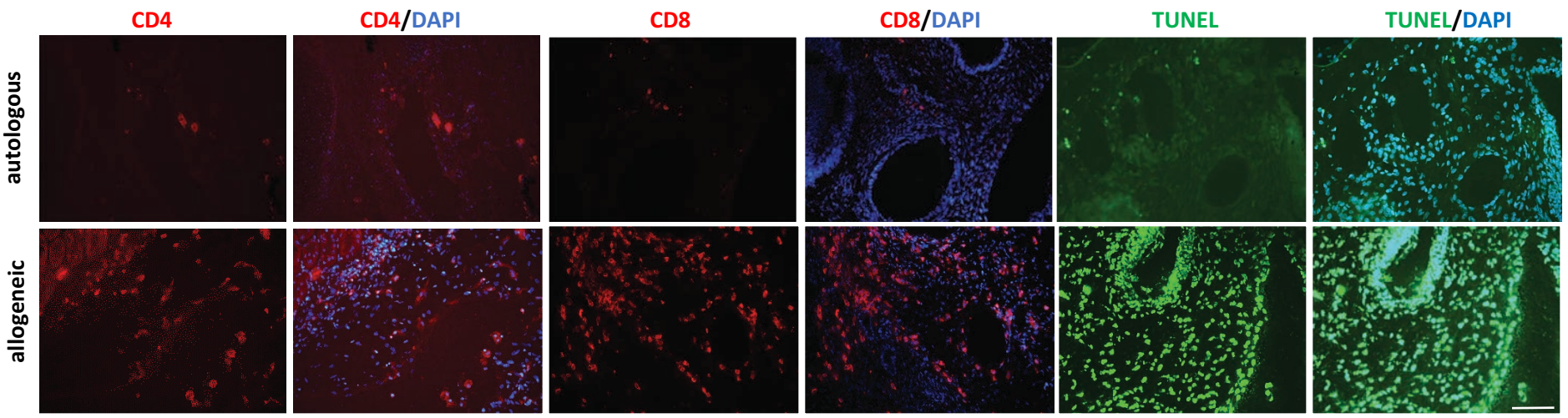

Benabdallah et al. Figure 4